

Received March 22, 2019, accepted April 10, 2019, date of publication April 22, 2019, date of current version May 2, 2019.

Digital Object Identifier 10.1109/ACCESS.2019.2912215

# Online Shape Modification of Molecular Weight Distribution Based on the Principle of Active Disturbance Rejection Controller

JING WANG<sup>ID</sup>, CHENGYUAN TAN, AND HAIYAN WU

College of Information Science and Technology, Beijing University of Chemical Technology, Beijing 100029, China

Corresponding author: Jing Wang (jwang@mail.buct.edu.cn)

This work was supported in part by the National Natural Science Foundation of China under Grant 61573050, in part by the Fundamental Research Funds for the Central Universities under Grant XK1802-4, and in part by the Open-Project Grant funded by the State Key Laboratory of Synthetical Automation for Process Industry at the Northeastern University under Grant PAL-N201702.

**ABSTRACT** Molecular weight distribution (MWD), an important microcosmic quality index of high polymer, is online unmeasurable, which makes its closed-loop control extremely difficult. To solve this problem, an online shape modification strategy for polymer MWD is proposed based on the active disturbance rejection controller (ADRC). The temporal-spatial property of MWD is estimated in real time by a three-layers forward network based on orthogonal polynomials basis function, and the shape modification of distribution function is transformed into the tracking control of moment statistics in the state-space description. Taking full advantage of the online measured lower-order moments, dual ADRCs are constructed with two manipulated variables (the flow rate of monomer and initiator) to achieve the high precision tracking of lower-order moments and distribution functions, simultaneously. Furthermore, the stability condition of the closed loop system is proved which can guide the parameter tuning of ADRCs. The proposed control strategy is implemented on the polymerization reaction in the laboratory scale continuous stirred tank reactor (CSTR). The feasibility and robustness are verified in the simulation.

**INDEX TERMS** Molecular weight distribution, active disturbance rejection controller, low-order moment, shape modification.

## I. INTRODUCTION

Polymers have played an increasingly important role in the chemical industry in recent decades. Different polymers have different properties, such as strength and thermal expansion. Its special microcosmic characteristics, such as molecular weight distribution (MWD) and particle size distribution, have significant influence on the end-use properties of polymer products. Therefore, it's very important to study the modeling and control of MWD and other similar characteristics [1], [2]. It's different from the ordinary chemical systems that the controlled variable in MWD control system is a distribution curve or probability density function (PDF) rather than a set point or a value, which means the control of MWD system is more complicated. At the same time, the lack of relevant online measuring techniques of MWD makes the

closed-loop control more difficult to achieve. Due to the complexity of the above problems, modeling and closed-loop control of MWD has become a great challenge.

At present, the main modeling method of MWD is completed by soft sensing, including mechanism modeling and data-driven modeling. Mechanism method is usually based on the reaction population balance to get a mathematical model composed of a set of high dimensional partial differential equations [3]–[6]. Researchers usually get suitable operation based on optimization methods [7], [8], but the large amount of calculation makes it difficult to be applied in practice. Data-driven modeling methods include neural network model [9], [10] and stochastic distribution system (SDC) whose system output is a probability density function [11], [12]. The traditional data model always is expressed as a simple state space description, and many effective control algorithms are put forward based on these data models to control the shape of PDF [13]–[17], [25].

The associate editor coordinating the review of this manuscript and approving it for publication was Ton Do.

Above controllers in [13]–[17] are designed only based on the data model without considering the process information, so they are implemented in open-loop form. The information of process should be feed back to controller. But the limitation of measurement techniques of MWD is existent. The Gel Permeation Chromatography(GPC) take a few dozen minutes or several hours to measure MWD [18], which means MWD can hardly be measured on-line. Therefore, other average indexes or variables should be controlled in the general polymerization process. Furthermore, since the existing data-driven model are constructed directly in a black box, it results that the model variables and control variables do not have clear physical meaning. For example, the state variables are just the weight vector of B-spline basis functions in [13]–[16]. Article proposes a neural network consisting of a series of orthogonal polynomial [19]. The most important is that the relation between the weights vector of the orthogonal polynomials function neural network and the MWD moments vector is proved. So the moments vector can be regarded as the state vector in the state space model. Better yet, the low order moments of MWD can be measured in real time [20], [21], so we can use the measured low order moments as the controlled variables to realize the online closed-loop control of the MWD shape.

ADRC was proposed based on PID principle by Han [22] and has many advantages in dealing with complex and nonlinear system. It contains 3 main parts: tracking differentiator (TD), state error feedback (SEF) and extended state observer (ESO). TD can change a step input into a smooth one for system, which can reduce the influence cause by big initial output error. It also can provide differential of input signal. ESO, the main part of ADRC, can accurately estimate the system uncertainty and external disturbance as total disturbance. SEF is the control law of ADRC, it use proportion and differentiation of the output error and disturbance compensation to get manipulating variable. ADRC can solve system disturbances very well, effectively control complex systems and has good adaptability and robustness, so it is widely use to control many kind of systems. Liu and Li use ADRC to control a planar motor speed system [23], and get a better dynamic performances when control with a sudden load and disturbances. ADRC was applied to control a multi-agent system with complex interconnection. The result shown that such disturbance can be actively estimated and canceled from each individual subsystem [24]. Powered parafoil system with strongly nonlinear and complicated cross-coupling can be effect control by ADRC in [26].

This paper will use the complex model in [19] to control the MWD shape. Considering the complexity and strong nonlinearity of the polymerization process and the inaccuracy of modeling, the design of controller still is a hard work. Many researches show that ADRC has strong ability to deal with complex systems and kinds of disturbances. Therefore, we want to use ADRC as controller in the MWD tracking control. Considering the practical situation, the model with uncertainty is

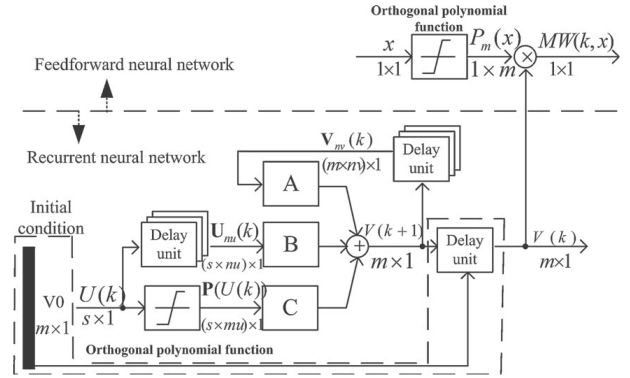


FIGURE 1. Structure of neural network.

used to test the robust performance of the controller in simulation.

The structure of this article is organized as follows. In section 2, the MWD model is constructed based on the orthogonal polynomials function neural network. Section 3 gives the online control scheme within the ADRC principle, and analyzes the stability of the control loop. Section 4 simulates the control schemes with the polystyrene reaction in the laboratory scale CSTR to analyze the feasibility and the robustness of the proposed method.

## II. NEURAL NETWORK MODEL

The orthogonal polynomials basis function based three-layers forward network is used to describe the space expansion property of MWD and the recurrent network is used to represent the time property in [19]. Fig. 1 gives the network structure. The state space description of model is as follows,

$$V(k+1) = AV_{nv}(k) + BU_{nu}(k) + CF(U(k)), \quad (1)$$

$$\gamma(k, x) = P \cdot V(k) = \sum_{i=1}^m v_i(k)p_i(x), \quad (2)$$

where  $A, B, C$  are weight matrices,  $m$  and  $s$  are the number of weight and input vector, respectively,  $V(k) = [v_1(k), v_2(k), \dots, v_m(k)]^T$  is the state,  $U(k) = [u_1(k), u_2(k), \dots, u_s(k)]^T$  is the input vector,  $P(x) = [p_1(x), p_2(x), \dots, p_m(x)]^T$  is orthogonal polynomials basis function,  $\gamma(k, x)$  is the output representing the concentration value of polymer macromolecule at sample time  $k$  with chain length  $x$ .  $V_{nv}(k)$ ,  $U_{nu}(k)$  and  $F(U(k))$  are block matrix, which can be expressed as follow,

$$V_{nv}(k) = [v^T(k), v^T(k-1), \dots, v^T(k-nv+1)]^T, \quad (3)$$

$$U_{nu}(k) = [U^T(k-1), U^T(k-2), \dots, U^T(k-nu)]^T, \quad (4)$$

$$F(U(k)) = [f(u_1(k)), f(u_2(k)), \dots, f(u_s(k))]^T, \quad (5)$$

where  $nu$  and  $nv$  are the input and output feedback order, respectively.  $f$  is the basis function of recurrent neural network, which can be orthogonal polynomial function or other function.

From [19], the linear mapping relationship between the low order MWD moment vector and the recurrent network weight vector  $V(k)$  is denoted as,

$$V(k) = G \cdot M(k), \quad (6)$$

where  $M(k) = [m_1, m_2, \dots, m_m]^T$  is the MWD order moment vector,  $m_1$  is 0<sup>th</sup> order moment,  $m_2$  is 1<sup>st</sup> order moment and so on. When the orthogonal polynomials basis function is determined, the transformational matrix  $G$  will be constant. Substituting (6) into (1) and (2), we get a new MWD model expressed as follow,

$$M(k+1) = \tilde{A}M_{nv}(k) + \tilde{B}U_{nu}(k) + \tilde{C}F(U(k)), \quad (7)$$

$$\gamma(k, x) = P \cdot G \cdot M(k), \quad (8)$$

where  $\tilde{A}$ ,  $\tilde{B}$ ,  $\tilde{C}$  are weight matrices and  $M_{nv}(k) = [M^T(k), M^T(k-1), \dots, M^T(k-nv+1)]^T$ .

The delay items of  $M(k)$  and  $U(k)$  in (7) have bad influence on controller design and stability analysis. Therefore, we want to change it to a new augmented system without delay.

Let  $\tilde{A} = [\tilde{a}_1, \tilde{a}_2, \dots, \tilde{a}_{nv}]$  and  $\tilde{B} = [\tilde{b}_1, \tilde{b}_2, \dots, \tilde{b}_{nu}]$ , where  $\tilde{a}_i$  and  $\tilde{b}_i$  are matrix with proper dimension. Then (7) can be rewritten as,

$$M(k+1) = \tilde{a}_1 M(k) + \dots + \tilde{a}_{nv} M(k-nv+1) + \tilde{b}_1 U(k-1) + \dots + \tilde{b}_{nu} U(k-nu) + \tilde{C}F(U(k)) \quad (9)$$

Define a new state variable as  $x(k) = [M^T(k-nv+1), M^T(k-nv+2), \dots, M^T(k)]^T$  and a new input variable as  $U_1(k) = [U^T(k-nu), U^T(k-nu+1), \dots, U^T(k-1)]^T$ , then we obtain a discrete system description without delay as follow,

$$x(k+1) = A_1 x(k) + B_1 U_1(k) + \tilde{F}(k), \quad (10)$$

where

$$A_1 = \begin{bmatrix} 0 & I & 0 & \dots & 0 \\ 0 & 0 & I & \dots & 0 \\ \vdots & \vdots & \vdots & \ddots & \vdots \\ 0 & 0 & 0 & \dots & I \\ \tilde{a}_{nv} & \tilde{a}_{nv-1} & \dots & \tilde{a}_2 & \tilde{a}_1 \end{bmatrix},$$

$$B_1 = \begin{bmatrix} 0 & 0 & 0 & \dots & 0 \\ 0 & 0 & 0 & \dots & 0 \\ \vdots & \vdots & \vdots & \ddots & \vdots \\ 0 & 0 & 0 & \dots & 0 \\ \tilde{b}_{nu} & \tilde{b}_{nu-1} & \dots & \tilde{b}_2 & \tilde{b}_1 \end{bmatrix}$$

and

$$\tilde{F}(k) = \begin{bmatrix} 0 \\ \vdots \\ 0 \\ \tilde{C}F(U(k)) \end{bmatrix}.$$

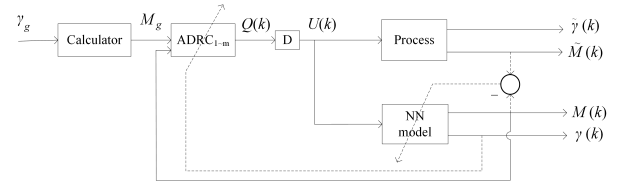


FIGURE 2. Structure of MWD control system.

### III. ONLINE TRACKING CONTROLLER DESIGN

#### A. SCHEME OF CONTROLLED SYSTEM

MWD can't be used as a feedback variable in on-line control system due to its large measurement delay. Low order moments have distinct physical meaning and are more easily measurable, and have a close relationship with MWD. Therefore, we use the low order moments of MWD as the controlled variables in the on-line control strategy.

When the orthogonal polynomials basis function is determined, output layer weight vector  $V$  can be directly calculated from the following equation [19],

$$v_{gi} = \frac{\sum_{x=1}^{\max l} \gamma_g(x) p_i(x)}{(p_i(x), p_i(x))}, i = 1, 2, \dots, m, \quad (11)$$

where  $l$  is the length of the polymer,  $v_{gi}$  is element of targeted weight vector  $V_g = [v_{g1}, v_{g2}, \dots, v_{gm}]^T$ ,  $\gamma_g(x)$  is the expected polymer concentration at chain length  $x$ . With the Eq.(6), we can get the targeted moment vector  $M_g$ . We can see that from the NN model, the influence of  $U(k)$  to output MWD is equal to the influence of  $U(k)$  to the moment vector  $M(k)$ . It means that the trace of target MWD can be changed by manipulating  $U(k)$  to make  $M(k)$  track the target moment vector  $M_g$ . The control of MWD is transformed into the control of  $M(k)$ .

The MWD control system is shown in Fig. 2. The output moment vector of network model,  $M(k)$  is send into controller as feedback variable. The information of NN model is used to adjust the controller, but the mismatch between the actual process and the network model will influence the control accuracy. A deviation  $e_M(k) = M(k) - \tilde{M}(k)$  between the output moment vector (real measurements) and the network estimations can be used to correct the network model.  $\tilde{M}(k)$  is the output moment vector of polymerization process.  $\gamma(k)$  and  $\tilde{\gamma}(k)$  is the output MWD of network model and actual process, respectively.  $\gamma_g$  is the reference MWD which is the desired polymer quality. Calculator computes the expected moment vector  $M_g$  from  $\gamma_g$  according to the (6) and (11). We design several individual ADRCs whose number is equal to the number of model weight vector. That means every ADRC respectively control a MWD moment. The output of  $i^{th}$  ADRC at time  $k$  is  $q_i(k)$ , which is the element of  $Q(k) = [q_1(k), q_2(k), \dots, q_m(k)]^T$ . Operating variable  $U(k)$  is computed from the following,

$$U(k) = DQ(k), \quad (12)$$

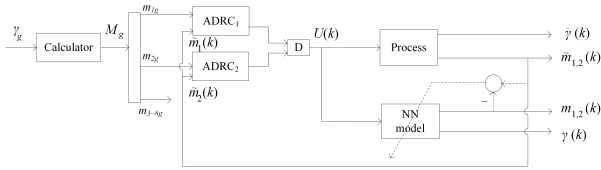


FIGURE 3. Simplified structure of MWD control system.

where  $D \in R^{s \times m}$  is weighting matrix, which can be shown as follow,

$$D = \begin{bmatrix} d_{11} & d_{12} & \cdots & d_{1m} \\ d_{21} & d_{22} & \cdots & d_{2m} \\ \vdots & \vdots & \ddots & \vdots \\ d_{s1} & d_{s2} & \cdots & d_{sm} \end{bmatrix}, \quad (13)$$

where  $\sum_{i=1}^m d_{ji}$  ( $j = 1, 2, \dots, s$ ). The value of  $d_{ji}$  reflects the importance of  $m_i(k)$  to input  $j$ , so we can adjust the weight of  $m_i(k)$  for control the shape of MWD by selecting the appropriate matrix  $D$ . We noticed that  $m$  equal to the number of moments in model, but the number of inputs  $s$  is always far smaller than  $m$ . Therefore, the system is under-actuated, which means the accurately control of every  $m_i(k)$  is difficult.

There are many controllers to be desired in the system mentioned above. Besides, the on-line correction of network model is too difficult to achieved. So we simplify the control structure and get a more simply achievable system.

It has been proved that the moments' free degrees of the distribution function are same as the number of its parameters. In other words, if we know how many parameters of a distribution function, we can determine the number of the controlled moments during the MWD control. Schulz distribution that has two parameters is used to describe MWD in the traditional chemical industrial process, so we can track the MWD shape by controlling 2 moments. Because the leading moments (lower order moments) of MWD can be measured on-line, so we choose  $m_1$  and  $m_2$ , the  $0^{th}$  and  $1^{st}$  order moments that can be measured on-line, as controlled variables in the simplified control system. So two ADRC controllers,  $ADRC_1$  and  $ADRC_2$ , are designed to control  $m_1$  and  $m_2$ , respectively. The number of ADRC reduces greatly that means the system in Fig. 3 is very simpler and more easily implemented than that of Fig. 2. Therefore, the weight matrix  $D$  should be changed to  $\tilde{D} \in R^{s \times 2}$ .

### B. CONTROLLER DESIGN

As we know, the deviation between the system model and the actual plant always exist, which will influence the control effect. Moreover, we need to consider the affect of the uncontrolled moments on the controlled moments in this simplified control scheme. So the extended state observer (ESO) is used to estimate all the above disturbances expressed as

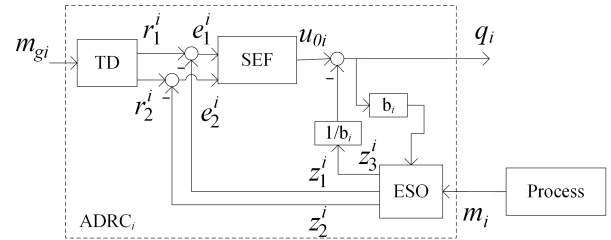


FIGURE 4. Structure of ADRC.

following,

$$\begin{cases} \varepsilon_0^i(k) = z_1^i(k) - m_i(k) \\ z_1^i(k+1) = z_1^i(k) + h(z_2^i(k) - \beta_1^i \varphi(\varepsilon_0^i(k), \alpha_1^i, \delta_1^i)) \\ z_2^i(k+1) = z_2^i(k) + h(z_3^i(k) - \beta_2^i \varphi(\varepsilon_0^i(k), \alpha_2^i, \delta_2^i) \\ + b_i q_i(k)) \\ z_3^i(k+1) = z_3^i(k) - h \beta_3^i \varphi(\varepsilon_0^i(k), \alpha_3^i, \delta_3^i) \end{cases} \quad (14)$$

$$\varphi(x, \alpha, \delta) = \begin{cases} x / \delta^{(1-\alpha)}, & |x| \leq \delta \\ \text{sign}(x) |x|^\alpha, & |x| > \delta. \end{cases}$$

where  $z_1^i$ ,  $z_2^i$  and  $z_3^i$  are the estimates of  $i^{th}$  moment, the moment's derivative and total disturbance.

Tracking differentiator (TD) designs a gentle transition process (doesn't like step) for the control system, which is represented as the following equations,

$$\begin{cases} r_1^i(k+1) = r_1^i(k) + h r_2^i(k) \\ r_2^i(k+1) = r_2^i(k) + h f_{st}(r_1^i(k) - \mu_{gi}(k), r_2^i(k), \delta_0^i, h_0^i) \\ d = \delta_0^i h_0^i, d_0 = d h_0^i \\ m^i = r_1^i(k) - \mu_{gi}(k) + h_0^i r_2^i(k), a_0 = (d^2 + 8 \delta_i |m^i|)^{\frac{1}{2}} \\ a = \begin{cases} r_2^i(k) + (a_0 - d) \text{sgn}(m^i) / 2, & |m^i| > d_0 \\ r_2^i(k) + m^i / h_0^i, & |m^i| \leq d_0 \end{cases} \\ f_{st} = - \begin{cases} \delta_0^i a / d, & |a| \leq d \\ \delta_0^i \text{sgn}(a), & |a| > d \end{cases} \end{cases} \quad (15)$$

The non-linear state error feedback (SEF) control law is design as follow,

$$\begin{cases} e_1^i(k) = r_1^i(k) - z_1^i(k) \\ e_2^i(k) = r_2^i(k) - z_2^i(k) \\ u_{0i}(k) = k_1^i e_1^i(k) + k_2^i e_2^i(k) \\ q_i(k) = u_{0i}(k) - z_3^i(k) / b_i. \end{cases} \quad (16)$$

Scheme of ADRC is shown in Fig. 4, and it comprises of the above parts (TD, SEF and ESO). All ADRCs in the MWD control system have the same structure.

### C. STABILITY ANALYSIS

In order to simplify the stability analysis, let the inputs of all ADRC  $m_{gi}$  ( $i = 1, 2, \dots, m$ ) are zero, so all the outputs of TD are also zero.

According to above assumption and (16), we can get

$$q_i(k) = -k_1^i z_1^i(k) - k_2^i z_2^i(k) - \frac{z_3^i(k)}{b_i}. \quad (17)$$

Substitute  $q_i(k)$  into (14), and let

$$z^i(k) = [z_1^i(k), z_2^i(k), z_3^i(k)]^T,$$

then we obtain

$$z^i(k+1) = B_4^i z^i(k) + h\varphi(\varepsilon_0^i(k)) B_5^i, \quad (18)$$

where

$$B_4^i = \begin{bmatrix} 1 & h & 0 \\ -hb_ik_1^i & 1 - hb_ik_2^i & 0 \\ 0 & 0 & 1 \end{bmatrix}, \quad B_5^i = \begin{bmatrix} -\beta_1^i \\ -\beta_2^i \\ -\beta_3^i \end{bmatrix}$$

So the state space model of all ESOs can be written as follow,

$$z(k+1) = \begin{bmatrix} B_4^1 & & & \\ & B_4^2 & & \\ & & \ddots & \\ & & & B_4^m \end{bmatrix} z(k) + h \begin{bmatrix} B_5^1 & & & \\ & B_5^2 & & \\ & & \ddots & \\ & & & B_5^m \end{bmatrix} w(k) \quad (19)$$

$$= B_4 z(k) + hB_5 w(k). \quad (20)$$

where

$$z(k) = \begin{bmatrix} z^1(k) \\ z^2(k) \\ \vdots \\ z^m(k) \end{bmatrix}, \quad w(k) = \begin{bmatrix} \varphi(\varepsilon_0^1(k)) \\ \varphi(\varepsilon_0^2(k)) \\ \vdots \\ \varphi(\varepsilon_0^m(k)) \end{bmatrix}$$

For replacing the  $U_1(k)$  in (10), define  $Z(k) = [z^T(k-nu), z^T(k-nu+1), \dots, z^T(k-1)]^T$ , and we obtain,

$$Z(k+1) = \begin{bmatrix} B_4 & & & \\ & B_4 & & \\ & & \ddots & \\ & & & B_4 \end{bmatrix} \begin{bmatrix} z(k-nu) \\ z(k-nu+1) \\ \vdots \\ z(k-1) \end{bmatrix} + h \begin{bmatrix} B_5 & & & \\ & B_5 & & \\ & & \ddots & \\ & & & B_5 \end{bmatrix} \begin{bmatrix} w(k-nu) \\ w(k-nu+1) \\ \vdots \\ w(k-1) \end{bmatrix} = B_6 Z(k) + hB_7 W(k). \quad (21)$$

Take single input as an example. Substituting  $q_i(k)$  into (12), we obtain

$$U(k) = \sum_{i=1}^m d_i q_i(k) = \sum_{i=1}^m d_i \left( -k_1^i z_1^i(k) - k_2^i z_2^i(k) - \frac{z_3^i(k)}{b_i} \right) = B_2 z(k). \quad (22)$$

where  $B_2 = [-d_1 k_1^1, -d_1 k_2^1, -d_1 b_1, \dots, -d_m k_1^m, -d_m k_2^m, -d_m b_m]$ .

Therefore,  $U_1(k)$  can be rewritten as follow,

$$U_1(k) = \begin{bmatrix} U(k-nu) \\ U(k-nu+1) \\ \vdots \\ U(k-1) \end{bmatrix} = \begin{bmatrix} B_2 & & & \\ & B_2 & & \\ & & \ddots & \\ & & & B_2 \end{bmatrix} \begin{bmatrix} z(k-nu) \\ z(k-nu+1) \\ \vdots \\ z(k-1) \end{bmatrix} = B_3 Z(k). \quad (23)$$

Substitute (23) into (10), then

$$x(k+1) = A_1 x(k) + B_1 B_3 Z(k) + \bar{F}(k). \quad (24)$$

Define  $X(k) = [x^T(k), Z^T(k)]^T$ . Combining (17) and (23), the whole closed loop system can be express as follow

$$X(k+1) = A_2 X(k) + B_8 W(k) + G(k), \quad (25)$$

where

$$A_2 = \begin{bmatrix} A_1 & B_1 B_3 \\ 0 & B_6 \end{bmatrix}, \quad B_8 = \begin{bmatrix} 0 \\ hB_7 \end{bmatrix}$$

and

$$G(k) = \begin{bmatrix} \bar{F}(k) \\ 0 \end{bmatrix}.$$

For proving the stability, a relationship between estimation error and  $W(k)$  is presented in following formula. Define  $y_i(k+1) = z_1^i(k) - m_i(k)$  and  $Y(k+1) = [y_1(k+1), y_2(k+1), \dots, y_m(k+1)]^T$ , and we have,

$$Y(k+1) = C_1 M(k) + C_2 z(k), \quad (26)$$

where

$$C_1 = \begin{bmatrix} -1 & & & \\ & -1 & & \\ & & \ddots & \\ & & & -1 \end{bmatrix}$$

and

$$C_2 = \begin{bmatrix} 1 & 0 & 0 & & & \\ & 1 & 0 & 0 & & \\ & & \ddots & & & \\ & & & 1 & 0 & 0 \end{bmatrix}.$$

With further deduction on (26), we obtain

$$Y(k+1) = C_1 \underbrace{\begin{bmatrix} 0 & \dots & 0 \\ \vdots & & \vdots \end{bmatrix}}_{m \times 1} I x(k) + C_2 \underbrace{\begin{bmatrix} 0 & \dots & 0 \\ \vdots & & \vdots \end{bmatrix}}_{nu \times 1} I Z(k+1)$$

$$\begin{aligned}
 &= C_1[\underbrace{0 \dots 0}_{mv-1} I]x(k) \\
 &\quad + C_2[\underbrace{0 \dots 0}_{nu-1} I][B_6Z(k) + hB_7Z(k)] \\
 &= C_3X(k) + C_4W(k), \tag{27}
 \end{aligned}$$

where

$$C_3 = \left[ C_1[\underbrace{0 \dots 0}_{mv-1} I], C_2[\underbrace{0 \dots 0}_{nu-1} I]B_6 \right]$$

and

$$C_4 = hC_2[\underbrace{0 \dots 0}_{nu-1} I]B_7.$$

Since  $x\varphi(x) > 0(x \neq 0)$ , so

$$Y^T(k+1)w(k) > 0. \tag{28}$$

Replace the  $w(k)$  in (28) by  $W(k+1)$ , and we obtain,

$$Y^T(k+1)w(k) = Y^T(k+1)C_5W(k+1) > 0, \tag{29}$$

where

$$C_5 = [\underbrace{0 \dots 0}_{nu-1} I].$$

The following theorem shows the stability of the closed-loop system.

*Theorem 1:* If a positive definite symmetric matrix  $P$  can satisfy the following condition is exist,

$$\begin{bmatrix} -P & C_3^T C_5 & P & A_2^T P \\ C_5^T C_3 & C_4^T C_5 + C_5^T C_4 & 0 & B_8^T P \\ P & 0 & -P & 0 \\ PA_2 & PB_8 & 0 & -P \end{bmatrix} < 0, \tag{30}$$

the closed-loop system (25) is stable and state error is bounded.

*Proof:* A Lyapunov function is chosen as,

$$\begin{aligned}
 E(k) &= [X(k) - G(k-1)]^T P [X(k) - G(k-1)] \\
 &\quad + 2 \sum_{n=1}^k Y^T(n) C_5 W(n). \tag{31}
 \end{aligned}$$

$$\begin{aligned}
 \Delta &= E(k+1) - E(k) \\
 &= X^T(k)A_2^T PA_2 X(k) + X^T(k)A_2^T PB_8 W(k) \\
 &\quad + W^T(k)B_8^T PA_2 X(k) + W^T(k)B_8^T PB_8 W(k) \\
 &\quad - X^T(k)PX(k) + X^T(k)PG(k-1) \\
 &\quad + G^T(k-1)PX(k) - G^T(k-1)PG(k-1) \\
 &\quad + [C_3X(k) + C_4W(k)]^T C_5 W(k) \\
 &\quad + W^T(k)C_5^T [C_3X(k) + C_4W(k)] \\
 &= X^T(k) \left( A_2^T PA_2 - P \right) X(k) + W^T(k) \left( B_8^T PB_8 \right. \\
 &\quad \left. + C_4^T C_5 + C_5^T C_4 \right) W(k) - G^T(k-1)PG(k-1) \\
 &\quad + X^T(k) \left( A_2^T PB_8 + C_3^T C_5 \right) W(k) \\
 &\quad + W^T(k) \left( B_8^T PA_2 + C_5^T C_3 \right) X(k) \\
 &\quad + X^T(k)PG(k-1) + G^T(k-1)PX(k) \tag{32}
 \end{aligned}$$

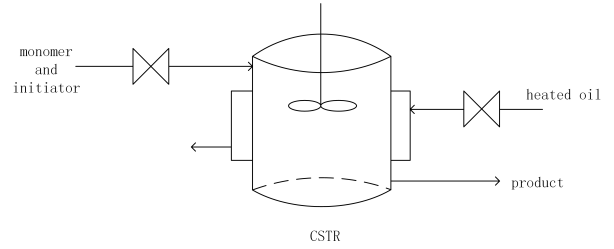


FIGURE 5. Structure of the laboratory scale CSTR.

Let  $S(k) = [X^T(k), W^T(k), G^T(k-1)]^T$ , so  $\Delta$  can be rewritten as,

$$\Delta = S^T \Phi S(k). \tag{33}$$

where

$$\Phi = \begin{bmatrix} A_2^T PA_2 - P & A_2^T PB_8 + C_3^T C_5 & P \\ B_8^T PA_2 + C_5^T C_3 & B_8^T PB_8 + C_4^T C_5 + C_5^T C_4 & 0 \\ P & 0 & -P \end{bmatrix}$$

$\Delta < 0$

can be transformed into  $\Phi < 0$ . According to the Schur complement theorem, we obtain

$$\Phi_1 = \begin{bmatrix} -P & C_3^T C_5 & P & A_2^T P \\ C_5^T C_3 & C_4^T C_5 + C_5^T C_4 & 0 & B_8^T P \\ P & 0 & -P & 0 \\ A_2 & B_8 & 0 & -P^{-1} \end{bmatrix} < 0. \tag{34}$$

Pre-multiply and post-multiply  $diag(I, I, I, P)$  to the left and right side of  $\Phi_1$ ,

$$\Phi_2 = \begin{bmatrix} -P & C_3^T C_5 & P & A_2^T P \\ C_5^T C_3 & C_4^T C_5 + C_5^T C_4 & 0 & B_8^T P \\ P & 0 & -P & 0 \\ PA_2 & PB_8 & 0 & -P \end{bmatrix} < 0. \tag{35}$$

Proof is completed. ■

#### IV. SIMULATION RESULT

In this section, laboratory scale continuously stirred tank reactor (CSTR), which is shown in Fig. 5 is used as controlled plant in simulation. The process is the free-radical solution polymerization of styrene in a jacketed continuous stirred tank reactor, while azobisisobutyronitrile (ABIN) is used as initiator. Two kinds of fluid, monomer and initiator, are added into the reactor through a control device. The heat of reaction is provided by the heated oil in jacket. The temperature of the oil is controlled by a temperature regulator to keep constant. The outlet flow is measured by a balance meter.

The polymerization mechanisms include four steps: initiation, chain propagation, chain transfer to monomer, and termination. The major ordinary differential equations (ODEs) are provided in the following to describe the polymerization process. The concentration of initiator  $I$ , monomer  $M$ , live polymer radical  $R$  and dead polymer  $P_j$  with chain length

TABLE 1. Parameters used in mechanism model.

Parameters	Values	Unit
$Ar_p$	$6.31 \times 10^8$	$l \cdot mol^{-1} \cdot min^{-1}$
$Ar_{trm}$	$1.38 \times 10^8$	$l \cdot mol^{-1} \cdot min^{-1}$
$Ar_t$	$3.76 \times 10^{10}$	$l \cdot mol^{-1} \cdot min^{-1}$
$Ar_d$	$9.48 \times 10^{16}$	$l \cdot mol^{-1} \cdot min^{-1}$
$E_p$	$7.06 \times 10^3$	$cal \cdot mol^{-1} \cdot K^{-1}$
$E_{trm}$	$1.26 \times 10^4$	$cal \cdot mol^{-1} \cdot K^{-1}$
$E_t$	$1.68 \times 10^3$	$cal \cdot mol^{-1} \cdot K^{-1}$
$E_d$	$3.08 \times 10^4$	$cal \cdot mol^{-1} \cdot K^{-1}$
$V$	3.927	$L$
$T$	353	$K$
$R$	1.987	$cal \cdot mol^{-1} \cdot L^{-1}$
$M^0$	4.81	$mol \cdot L^{-1}$
$I^0$	0.0106	$mol \cdot L^{-1}$
$f$	0.62	

$j$  are described as

$$\begin{aligned} \frac{dI}{dt} &= \frac{F}{V}(I^0 - I) - K_d I \\ \frac{dM}{dt} &= \frac{F}{V}(M^0 - M) - 2fK_d I - (K_p + K_{trm})RM \\ \frac{dR}{dt} &= -\frac{F}{V}R + 2fK_d I - K_t R^2 \\ \frac{dP_j}{dt} &= \frac{F}{V}(K_{trm}MR_1\alpha^{-(j-1)} + 0.5(j-1)K_t R_1^2\alpha^{-(j-2)} - P_j) \end{aligned} \quad (36)$$

where  $R_1$  and  $\alpha$  express as

$$\begin{aligned} R_1 &= \frac{2fK_d I + K_{trm}RM}{K_p M \alpha} \\ \alpha &= 1 + \frac{K_{trm}}{K_p} + \frac{K_t R}{K_p M} + \frac{F}{K_p MV} \end{aligned}$$

where  $V$  is the volume of CSTR,  $F$  represent input flow rate,  $I^0$  and  $M^0$  are initial concentrations of initiator and monomer in the input flow, respectively,  $f$  is the initiation efficiency.  $K_d$  is the initiator decomposition rate constant,  $K_p$  is the propagation rate constant,  $K_{trm}$  is the chain transfer rate constant,  $K_t$  is the termination rate constant. These rate constants  $K$  conform to the Arrhenius equation,

$$K_i = Ar_i e^{-\frac{E_i}{RT}}, \quad (37)$$

where subscript  $i$  represents different polymerization process,  $i \in \{d, p, trm, t\}$ .  $Ar$  is pre-exponential factor,  $E$  is activation energy,  $R$  is molar gas constant and  $T$  is reaction temperature. Table 1 shows parameters used in mechanism model.

The MWD of reaction product polystyrene is output. The maximum polymer chain length is  $maxl = 2000$ , and the dimensionality of the moment vector  $M(k)$  is  $m = 8$ . The inputs are flow rates of monomer and initiator, both of their range are  $[9.52, 14.28]$ . So the input dimensionality is  $s = 2$ , beside  $\tilde{D} \in R^{2 \times 2}$ . The weighting matrix  $\tilde{D}$  is chosen as

$$\tilde{D} = \begin{bmatrix} 0.7 & 0.3 \\ 0.2 & 0.8 \end{bmatrix}.$$

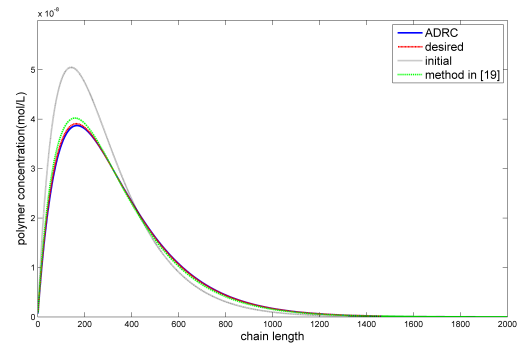


FIGURE 6. Track to the desired MWD at final time under different control methods.

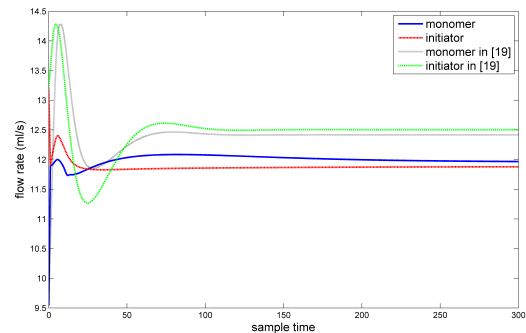


FIGURE 7. Manipulated variables under different control methods.

The sum of square error between output MWD of process and the desired MWD is shown as follow,

$$e(k) = \sum_{x=1}^{maxl} (\gamma(k, x) - \gamma_g(x))^2, \quad k = 1, 2, \dots, N, \quad (38)$$

where  $N = 300$  is the final sample time, sampling interval is 1 min. The sum of whole controlled process error expressed as,

$$E = \sum_{k=1}^N e(k). \quad (39)$$

We use the proposed method to realize the MWD control of polystyrene in CSTR and compare with the method in [19], which carried out control strategy though optimizing a tracking performance function. Table 2 shows the parameters of the ADRC. The ADRC is adaptable and robust, so same parameters are set for both ADRCs for convenience. The following results are the track of desired MWD. Fig. 6 is tracking result to the desired MWD under different method at final sample time. Fig. 7 is variation of the flow rate under the different methods. Fig. 8 is dynamic 3-D variation of MWD under ADRC control.

Error index  $e(k)$  under two different control strategy are shown in Fig. 9. The  $e(k)$  of this work is  $6.49 \times 10^{-17}$  at final sample time, which is much smaller than error of [19] ( $4.36 \times 10^{-16}$ ). The  $E$  of this work ( $1.23 \times 10^{-13}$ ) is also smaller than [19] ( $3.03 \times 10^{-13}$ ). It can be seen that the effect of ADRC control is much better in situation of dynamic and steady.

TABLE 2. Parameters of ADRC.

Parameter	$\delta_0$	$h_0$	$\alpha_{01}$	$\alpha_{02}$	$\alpha_{03}$	$h$	$\beta_1$	$\beta_2$
Value	3	1	0.5	0.5	0.75	0.03	5	0.5
Parameter	$\beta_3$	$b$	$k_1$	$k_2$	$\delta_1$	$\delta_2$	$\delta_3$	
Value	0.1	0.25	0.4	0.6	0.05	0.03	0.01	

TABLE 3. Results of robust test.

activation energy of different reaction	Initiation $E_d$	Propagation $E_p$	Transfer $E_{trm}$	Termination $E_t$
normal value( $10^4$ )	3.08	0.706	1.26	0.168
changed value( $10^4$ )	3.076	0.709	1.23	0.165
$\bar{e}(10^{-16})$	6.26	4.75	2.93	1.11
$e_{ADRC}(10^{-16})$	6.90	2.17	2.48	0.756
$e_{[19]}(10^{-16})$	16.0	18.9	14.2	9.59
$E_{ADRC}(10^{-13})$	3.08	1.58	1.65	1.29
$E_{[19]}(10^{-13})$	6.39	7.18	5.81	4.32

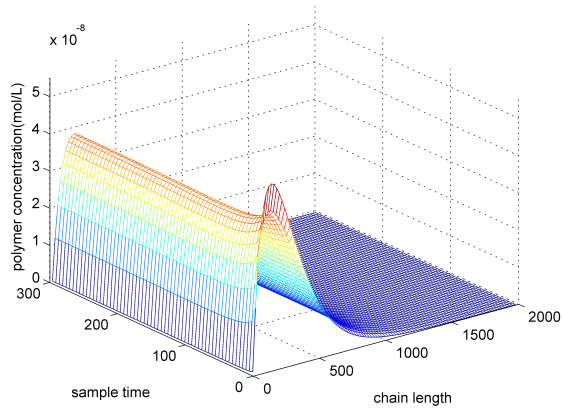


FIGURE 8. Variation of MWD under ADRC control.

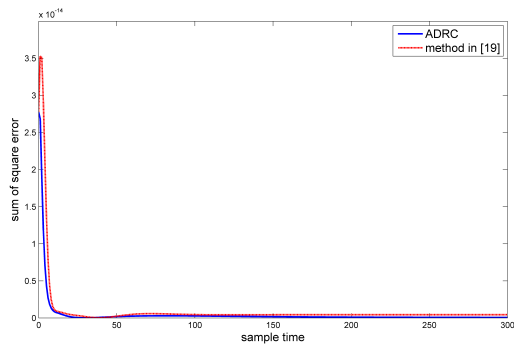


FIGURE 9. Comparison of  $e(k)$  between ADRC and the method in [19].

The changing of every element of moment vector under the different methods is shown in Fig. 10. Proposed method control the MWD moments more accurate and has a better dynamic process. But we can see that some moments, especially 2<sup>nd</sup> order moment, still can't accurately track the desired value. The under-actuated and complex make the accurately control of every moment too difficult to achieve.

To test the robustness of the controlled system, some parameters of the mechanism model are changed (only change a value at once), which causes the mismatch between

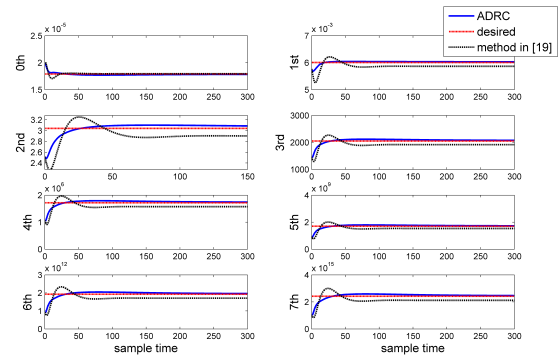


FIGURE 10. Variation of each order moment.

the model and the process. In other words, it tests the ability of the controller deal with model uncertainty. The parameters drift and control results are shown in Table 3.  $e_{\bullet}$  and  $E_{\bullet}$ , calculated by (38) and (39), are tracking error with parameters' drift at final sample time and whole process. The subscript  $\bullet$  means the method of control, ADRC or method in [19].  $\bar{e}$  is sum of square error between normal and drifted process output MWD at steady state with same input (values get from previously ADRC controlled input at  $k = N$ ), can be expressed as

$$\bar{e} = \sum_{x=1}^{\max l} (\gamma_d(x) - \gamma_g(x))^2, \quad (40)$$

where  $\gamma_d$  is the output MWD of drifted process.

Different parameters have different influence on polymerization.  $E_d$  is a more sensitive parameter than others for polymerization process, so we just make a little change to it. Table 3 is shown that ADRC can control the system with better effect when parameters drifted. Degree of error reduction between  $\bar{e}$  and  $e_{ADRC}$  is different with change of different parameters. Maybe the influence of change of  $E_p$  has stronger relationship with the controlled moments than other parameters, so the ability of resist  $E_p$  drifted is better. Because the drift of  $E_d$  influence whole process, the ADRC



control is no effect in this situation. We can see that ADRC has strong robustness.

## V. CONCLUSIONS

The effort of this work is proposing a control strategy of MWD, which makes MWD can be controlled on-line and track desired shape with ADRC. It solves the difficulty of on-line control of MWD. A theorem was proposed to discuss the stability of the controlled system, which can be used to determine the parameters of the controller. From the simulation, we can see that the output MWD of the polymerization process can be controlled as close as the desired curve. When mechanism parameters have changed, the system output still can track the desired MWD with a better quality. It means the system has robustness, which makes a good benefit for practice. How to improve the effect of controller on resisting disturbance is future work.

## REFERENCES

- [1] C. Kiparissides, "Challenges in particulate polymerization reactor modeling and optimization: A population balance perspective," *J. Process Control*, vol. 16, no. 3, pp. 205–224, Mar. 2006.
- [2] J. Kang, Z. Shao, X. Chen, X. Gu, and L. Feng, "Fast and reliable computational strategy for developing a rigorous model-driven soft sensor of dynamic molecular weight distribution," *J. Process Control*, vol. 56, no. 3, pp. 79–99, Aug. 2017.
- [3] N. Yaghini and P. D. Iedema, "Population balance modeling of full two-dimensional molecular weight and branching distributions for ldPE with topological scission in continuous stirred tank reactor," *Chem. Eng. Sci.*, vol. 137, no. 6, pp. 556–571, Dec. 2015.
- [4] A. Alshaiban and J. B. P. Soares, "Mathematical modeling of the microstructure of poly(propylene) made with ziegler-natta catalysts in the presence of electron donors," *Macromolecular Reaction Eng.*, vol. 5, no. 2, pp. 96–116, Feb. 2011.
- [5] R. C. Hiorns, A. Khoukh, P. Ghigo, S. Prim, and J. François, "A convenient route to high molecular weight highly isotactic polystyrene using Ziegler-Natta catalysts and ultrasound," *Polymer*, vol. 43, no. 11, pp. 3365–3369, May 2017.
- [6] Y.-C. Si, C.-K. Xie, and N. Zhao, "Boundary control for a class of reaction-diffusion systems," *Int. J. Autom. Comput.*, vol. 15, no. 1, pp. 94–102, Feb. 2018.
- [7] J. Weng et al., "A novel strategy for dynamic optimization of grade transition processes based on molecular weight distribution," *Aiche J.*, vol. 60, no. 7, pp. 2498–2512, Jul. 2014.
- [8] C. Zhang, J. Shao, X. Chen, X. Gu, L. Feng, and L. T. Biegler, "Optimal flowsheet configuration of a polymerization process with embedded molecular weight distributions," *Aiche J.*, vol. 62, no. 1, pp. 131–145, Jan. 2016.
- [9] S. Curteanu and F. Leon, "Optimization strategy based on genetic algorithms and neural networks applied to a polymerization process," *Int. J. Quantum Chem.*, vol. 108, no. 4, pp. 617–630, 2008.
- [10] A. L. Nogueira, L. M. F. Lona, and R. A. F. Machado, "Continuous polymerization in tubular reactors with prepolymerization: Analysis using two-dimensional phenomenological model and hybrid model with neural networks," *J. Appl. Polymer Sci.*, vol. 91, no. 2, pp. 871–882, Jan. 2004.
- [11] H. Wang, "Control of the output probability density functions for a class of nonlinear stochastic systems," *IFAC Proc. Vol.*, vol. 31, no. 4, pp. 95–99, Apr. 1998.
- [12] J. L. Zhou, H. Yue, J. F. Zhang, and H. Wang, "Iterative learning double closed-loop structure for modeling and controller design of output stochastic distribution control systems," *IEEE Trans. Control Syst. Technol.*, vol. 22, no. 6, pp. 2261–2276, Nov. 2014.
- [13] H. Yue, J. L. Zhou, and H. Wang, "Minimum entropy of B-spline PDF systems with mean constraint," *Automatica*, vol. 42, no. 6, pp. 989–994, Jun. 2006.
- [14] J. L. Zhou, G. T. Li, and H. Wang, "Robust tracking controller design for non-Gaussian singular uncertainty stochastic distribution systems," *Automatica*, vol. 50, no. 4, pp. 1296–1303, Apr. 2014.
- [15] J. F. Zhang, H. Yue, and J. Zhou, "Predictive PDF control in shaping of molecular weight distribution based on a new modeling algorithm," *J. Process Control*, vol. 30, no. 12, pp. 80–89, Jun. 2015.
- [16] L. N. Yao and L. Feng, "Fault diagnosis and fault tolerant tracking control for the non-Gaussian singular time-delayed stochastic distribution system with PDF approximation error," *Neurocomputing*, vol. 175, no. 2, pp. 538–543, Jun. 2016.
- [17] T.-R. Zong, Y. Xiang, S. Elbadry, and S. Nahavandi, "Modified moment-based image watermarking method robust to cropping attack," *Int. J. Autom. Comput.*, vol. 13, no. 3, pp. 259–267, Jun. 2016.
- [18] J. C. Moore, "Gel permeation chromatography. I. A new method for molecular weight distribution of high polymers," *J. Polymer Sci. Part A, Polymer Chem.*, vol. 34, no. 10, pp. 1833–1841, Jul. 1996.
- [19] H. Wu, L. Cao, and J. Wang, "Gray-box modeling and control of polymer molecular weight distribution using orthogonal polynomial neural networks," *J. Process Control*, vol. 22, no. 9, pp. 1624–1636, Oct. 2012.
- [20] S. Ponnuswamy, S. L. Shah, and C. Kiparissides, "On-line monitoring of MWD in a batch polymerization reactor by size exclusion chromatography," *J. Liq. Chromatography*, vol. 9, no. 11, pp. 2411–2423, Sep. 1986.
- [21] F. J. Schork et al., "Miniemulsion polymerization," *Polymer Particles*, vol. 175, pp. 129–255, Feb. 2005.
- [22] J. Han, "From PID to active disturbance rejection control," *IEEE Trans. Ind. Electron.*, vol. 56, no. 3, pp. 900–906, Mar. 2009.
- [23] X. M. Liu and X. F. Li, "Application of an auto-disturbance rejection controller in planar motor speed control system," *Appl. Mech. Mater.*, vols. 462–463, no. 2, pp. 761–765, 2014.
- [24] H. Sira-Ramírez, Z. Q. Gao, and E. Canuto, "An active disturbance rejection control approach for decentralized tracking in interconnected systems," in *Proc. Eur. Control Conf.*, Strasbourg, France, Jun. 2014, pp. 588–593.
- [25] G.-H. Lin, J. Zhang, and Z.-H. Liu, "Hybrid particle swarm optimization with differential evolution for numerical and engineering optimization," *Int. J. Autom. Comput.*, vol. 15, no. 1, pp. 103–114, Feb. 2018.
- [26] S. Luo et al., "On decoupling trajectory tracking control of unmanned powered parafoil using ADRC-based coupling analysis and dynamic feed-forward compensation," *Nonlinear Dyn.*, vol. 92, no. 4, pp. 1619–1635, Jun. 2018.



**JING WANG** was born in Tangshang, Hebei, China, in 1972. She received the B.S. degree in industry automation and the Ph.D. degree in control theory and control engineering from Northeastern University, China, in 1994 and 1998, respectively.

She is currently a Professor with the College of Information Science and Technology, Beijing University of Chemical Technology University, China. Her research interests include complex systems, process monitoring, fault detection and diagnosis, and advance control.



**CHENGYUAN TAN** was born in Liuzhou, Guangxi, China, in 1994. He received the B.S. degree in automation from the Beijing University of Chemical Technology, China, in 2012, where he is currently pursuing the M.S. degree in control science and control engineering.

His research interests include active disturbance rejection controller and iterative learning control.



**HAIYAN WU** received the B.E. degree in industrial automation and the M.E. and Ph.D. degrees in control theory and control engineering from the Beijing University of Chemical Technology, China, in 2001, 2004, and 2012, respectively.

She is currently an Associate Professor with the College of Information Science and Technology, Beijing University of Chemical Technology. Her research interests include complex systems, fault detection and diagnosis, data mining and analytic, and machine learning.